

# Evaluation of Non-Intrusive Approaches for Wiener-Askey Generalized Polynomial Chaos

M. S. Eldred\*     C. G. Webster<sup>†</sup>

*Sandia National Laboratories<sup>‡</sup>, Albuquerque, NM 87185*

P. G. Constantine<sup>§</sup>

*Stanford University, Stanford, CA 94305*

Polynomial chaos expansions (PCE) are an attractive technique for uncertainty quantification (UQ) due to their strong mathematical basis and ability to produce functional representations of stochastic variability. When tailoring the orthogonal polynomial bases to match the forms of the input uncertainties in a Wiener-Askey scheme, excellent convergence properties can be achieved for general probabilistic analysis problems. Non-intrusive PCE methods allow the use of simulations as black boxes within UQ studies, and involve the calculation of chaos expansion coefficients based on a set of response function evaluations. These methods may be characterized as being either Galerkin projection methods, using sampling or numerical integration, or regression approaches (also known as point collocation or stochastic response surfaces), using linear least squares. Numerical integration methods may be further categorized as either tensor product quadrature or sparse grid Smolyak cubature and as either isotropic or anisotropic. Experience with these approaches is presented for algebraic and PDE-based benchmark test problems, demonstrating the need for accurate, efficient coefficient estimation approaches that scale for problems with significant numbers of random variables.

## I. Introduction

Uncertainty quantification (UQ) is the process of determining the effect of input uncertainties on response metrics of interest. These input uncertainties may be characterized as either aleatory uncertainties, which are irreducible variabilities inherent in nature, or epistemic uncertainties, which are reducible uncertainties resulting from a lack of knowledge. Since sufficient data is generally available for aleatory uncertainties, probabilistic methods are commonly used for computing response distribution statistics based on input probability distribution specifications. Conversely, for epistemic uncertainties, data is generally sparse, making the use of probability theory questionable and leading to nonprobabilistic methods based on interval specifications.

In this work, we focus on the analysis of aleatory uncertainties using the polynomial chaos expansion (PCE) approach to UQ. In particular, we focus on generalized polynomial chaos using the Wiener-Askey scheme,<sup>1</sup> in which Hermite, Legendre, Laguerre, Jacobi, and generalized Laguerre orthogonal polynomials are used for modeling the effect of continuous random variables described by normal, uniform, exponential, beta, and gamma probability distributions, respectively<sup>a</sup>. These orthogonal polynomial selections are optimal for these distribution types since the inner product weighting function and its corresponding support range correspond to the probability density functions for these continuous distributions. In theory, exponential convergence rates can be obtained with the optimal basis. When transformations to independent standard

---

\*Principal Member of Technical Staff, Optimization and Uncertainty Estimation Department, MS-1318, Associate Fellow AIAA.

<sup>†</sup>John von Neumann Fellow, Optimization and Uncertainty Estimation Department, MS-1318.

<sup>‡</sup>Sandia is a multiprogram laboratory operated by Sandia Corporation, a Lockheed Martin Company, for the United States Department of Energy's National Nuclear Security Administration under Contract DE-AC04-94AL85000.

<sup>§</sup>Ph.D. candidate, Institute for Computational and Mathematical Engineering.

<sup>a</sup>Orthogonal polynomial selections also exist for discrete probability distributions, but are not explored here.

random variables (in some cases, approximated by uncorrelated standard random variables) are used, the variable expansions are uncoupled, allowing the polynomial orthogonality properties to be applied on a per-dimension basis. This allows one to mix and match the polynomial basis used for each variable without interference with the Galerkin projection scheme for the response.

In non-intrusive PCE, simulations are used as black boxes and the calculation of chaos expansion coefficients for response metrics of interest is based on a set of simulation response evaluations. To calculate these response PCE coefficients, two primary classes of approaches have been proposed: Galerkin projection and linear regression. The Galerkin projection approach projects the response against each basis function using inner products and employs the polynomial orthogonality properties to extract each coefficient. Each inner product involves a multidimensional integral over the support range of the weighting function, which can be evaluated numerically using quadrature, cubature, or sampling approaches. The linear regression approach (also known as point collocation or stochastic response surfaces) uses a single linear least squares solution to solve for the PCE coefficients which best match a set of response values obtained from a design of computer experiments.

Section II describes the generalized polynomial chaos process in additional detail, Section III describes non-intrusive approaches for calculating the polynomial chaos coefficients, Section IV presents computational results, and Section V provides concluding remarks.

## II. Generalized Polynomial Chaos

### A. Askey scheme

Table 1 shows the set of polynomials which provide an optimal basis for different continuous probability distribution types. It is derived from the family of hypergeometric orthogonal polynomials known as the Askey scheme,<sup>2</sup> for which the Hermite polynomials originally employed by Wiener<sup>3</sup> are a subset. The optimality of these basis selections derives from the use of inner product weighting functions that correspond to the probability density functions (PDFs) of the continuous distributions when placed in a standard form. The density and weighting functions differ by a constant factor due to the requirement that the integral of the PDF over the support range is one.

**Table 1. Linkage between standard forms of continuous probability distributions and Askey scheme of continuous hyper-geometric polynomials.**

Distribution	Density function	Polynomial	Weight function	Support range
Normal	$\frac{1}{\sqrt{2\pi}} e^{-\frac{x^2}{2}}$	Hermite $He_n(x)$	$e^{-\frac{x^2}{2}}$	$[-\infty, \infty]$
Uniform	$\frac{1}{2}$	Legendre $P_n(x)$	1	$[-1, 1]$
Beta	$\frac{(1-x)^\alpha(1+x)^\beta}{2^{\alpha+\beta+1}B(\alpha+1,\beta+1)}$	Jacobi $P_n^{(\alpha,\beta)}(x)$	$(1-x)^\alpha(1+x)^\beta$	$[-1, 1]$
Exponential	$e^{-x}$	Laguerre $L_n(x)$	$e^{-x}$	$[0, \infty]$
Gamma	$\frac{x^\alpha e^{-x}}{\Gamma(\alpha+1)}$	Generalized Laguerre $L_n^{(\alpha)}(x)$	$x^\alpha e^{-x}$	$[0, \infty]$

Note that Legendre is a special case of Jacobi for  $\alpha = \beta = 0$ , Laguerre is a special case of generalized Laguerre for  $\alpha = 0$ , the Beta function is defined as  $B(a, b) = \frac{\Gamma(a)\Gamma(b)}{\Gamma(a+b)}$ , and the Gamma function  $\Gamma(a)$  is an extension of the factorial function to real values. Some care is necessary when specifying the  $\alpha$  and  $\beta$  parameters for the Jacobi and generalized Laguerre polynomials since the orthogonal polynomial conventions<sup>4</sup> differ from the common statistical PDF conventions. The former conventions are used in Table 1.

### B. Polynomial Chaos

The set of polynomials from Section II.A are used as an orthogonal basis to approximate the functional form between the stochastic response output and each of its random inputs. The chaos expansion for a response  $R$  takes the form

$$R = a_0 B_0 + \sum_{i_1=1}^{\infty} a_{i_1} B_1(\xi_{i_1}) + \sum_{i_1=1}^{\infty} \sum_{i_2=1}^{i_1} a_{i_1 i_2} B_2(\xi_{i_1}, \xi_{i_2}) + \sum_{i_1=1}^{\infty} \sum_{i_2=1}^{i_1} \sum_{i_3=1}^{i_2} a_{i_1 i_2 i_3} B_3(\xi_{i_1}, \xi_{i_2}, \xi_{i_3}) + \dots \quad (1)$$

where each additional set of nested summations indicates an additional order of polynomials in the expansion. This expression can be simplified by reformulating from an order-based indexing to a term-based indexing

$$R = \sum_{j=0}^{\infty} \alpha_j \Psi_j(\boldsymbol{\xi}) \quad (2)$$

where there is a one-to-one correspondence between  $a_{i_1 i_2 \dots i_n}$  and  $\alpha_j$  and between  $B_n(\xi_{i_1}, \xi_{i_2}, \dots, \xi_{i_n})$  and  $\Psi_j(\boldsymbol{\xi})$ . Each of the  $\Psi_j(\boldsymbol{\xi})$  are multivariate polynomials which involve products of the one-dimensional polynomials. For example, a multivariate Hermite polynomial  $B(\boldsymbol{\xi})$  of order  $n$  is defined from

$$B_n(\xi_{i_1}, \dots, \xi_{i_n}) = e^{\frac{1}{2}\boldsymbol{\xi}^T \boldsymbol{\xi}} (-1)^n \frac{\partial^n}{\partial \xi_{i_1} \dots \partial \xi_{i_n}} e^{-\frac{1}{2}\boldsymbol{\xi}^T \boldsymbol{\xi}} \quad (3)$$

which can be shown to be a product of one-dimensional Hermite polynomials involving a multi-index  $m_i^j$ :

$$B_n(\xi_{i_1}, \dots, \xi_{i_n}) = \Psi_j(\boldsymbol{\xi}) = \prod_{i=1}^n \psi_{m_i^j}(\xi_i) \quad (4)$$

The first few multidimensional Hermite polynomials for a two-dimensional case (covering zeroth, first, and second order terms) are then

$$\begin{aligned} \Psi_0(\boldsymbol{\xi}) &= \psi_0(\xi_1) \psi_0(\xi_2) = 1 \\ \Psi_1(\boldsymbol{\xi}) &= \psi_1(\xi_1) \psi_0(\xi_2) = \xi_1 \\ \Psi_2(\boldsymbol{\xi}) &= \psi_0(\xi_1) \psi_1(\xi_2) = \xi_2 \\ \Psi_3(\boldsymbol{\xi}) &= \psi_2(\xi_1) \psi_0(\xi_2) = \xi_1^2 - 1 \\ \Psi_4(\boldsymbol{\xi}) &= \psi_1(\xi_1) \psi_1(\xi_2) = \xi_1 \xi_2 \\ \Psi_5(\boldsymbol{\xi}) &= \psi_0(\xi_1) \psi_2(\xi_2) = \xi_2^2 - 1 \end{aligned}$$

A generalized polynomial basis is generated by selecting the univariate basis that is most optimal for each random input and then applying the products as defined by the multi-index to define a mixed set of multivariate polynomials. Similarly, the multivariate weighting functions involve a product of the one-dimensional weighting functions and the multivariate quadrature rules involve a tensor product of the one-dimensional quadrature rules. The use of independent standard random variables is the critical component that allows decoupling of the multidimensional integrals in a mixed basis expansion. It is assumed in this work that the uncorrelated standard random variables resulting from the transformation described in Section II.C can be treated as independent. This assumption is valid for uncorrelated standard normal variables (and motivates the popular approach of using a strictly Hermite basis), but is an approximation for uncorrelated standard uniform, exponential, beta, and gamma variables. For independent variables, the multidimensional integrals involved in the inner products of multivariate polynomials decouple to a product of one-dimensional integrals involving only the particular polynomial basis and corresponding weight function selected for each random dimension. The multidimensional inner products are nonzero only if each of the one-dimensional inner products is nonzero, which preserves the desired multivariate orthogonality properties for the case of a mixed basis.

In practice, one truncates the infinite expansion at a finite number of random variables and a finite expansion order

$$R = \sum_{j=0}^P \alpha_j \Psi_j(\boldsymbol{\xi}) \quad (5)$$

where the total number of terms  $N$  in a complete polynomial chaos expansion of arbitrary order  $p$  for a response function involving  $n$  uncertain input variables is given by

$$N = 1 + P = 1 + \sum_{s=1}^p \frac{1}{s!} \prod_{r=0}^{s-1} (n+r) = \frac{(n+p)!}{n!p!} \quad (6)$$

### C. Transformations to uncorrelated standard variables

Polynomial chaos is expanded using orthogonal polynomials which are functions of independent standard random variables  $\boldsymbol{\xi}$ . The dimension of  $\boldsymbol{\xi}$  is typically chosen to correspond to the dimension of the original random variables  $\mathbf{x}$ , although this is not required. In fact, the dimension of  $\boldsymbol{\xi}$  should be chosen to represent the number of distinct sources of randomness in a particular problem, and if individual  $x_i$  mask multiple random inputs, then the dimension of  $\boldsymbol{\xi}$  can be expanded to accommodate. For simplicity, all subsequent discussion will assume a one-to-one correspondence between  $\boldsymbol{\xi}$  and  $\mathbf{x}$ .

This notion of uncorrelated standard space is extended over the notion of “u-space” used in reliability methods<sup>5,6</sup> in that it includes not just uncorrelated standard normals, but also uncorrelated standardized uniforms, exponentials, betas and gammas. For problems directly involving independent normal, uniform, exponential, beta, and gamma distributions for input random variables, conversion to standard form involves a simple linear scaling transformation (to the form of the density functions in Table 1) and then the corresponding chaos can be employed. For correlated normal, uniform, exponential, beta, and gamma distributions, the same linear scaling transformation is applied followed by application of the inverse Cholesky factor of the correlation matrix (similar to Eq. 8 below, but the correlation matrix requires no modification for linear transformations). As described previously, the subsequent independence assumption is valid for uncorrelated standard normals but introduces error for uncorrelated standard uniform, exponential, beta, and gamma variables. For other distributions with a close explicit relationship to variables supported in the Askey scheme (i.e., lognormals and loguniforms), a nonlinear transformation is employed to transform to the corresponding Askey distributions (i.e., normals and uniforms) and the corresponding chaos polynomials (i.e., Hermite and Legendre) are employed. For other less directly-related distributions (e.g., extreme value distributions), the nonlinear Nataf transformation is employed to transform to uncorrelated standard normals as described below and Hermite chaos is employed. Future work will explore nonlinear transformations to other standard variables that allow a better match between the original distribution and the support ranges shown in Table 1.

The transformation from correlated non-normal distributions to uncorrelated standard normal distributions is denoted as  $\mathbf{u} = T(\mathbf{x})$  with the reverse transformation denoted as  $\mathbf{x} = T^{-1}(\mathbf{u})$ . These transformations are nonlinear in general, and possible approaches include the Rosenblatt,<sup>7</sup> Nataf,<sup>8</sup> and Box-Cox<sup>9</sup> transformations. The nonlinear transformations may also be linearized, and common approaches for this include the Rackwitz-Fiessler<sup>10</sup> two-parameter equivalent normal and the Chen-Lind<sup>11</sup> and Wu-Wirsching<sup>12</sup> three-parameter equivalent normals. The results in this paper employ the Nataf nonlinear transformation, which is suitable for the common case when marginal distributions and a correlation matrix are provided, but full joint distributions are not known<sup>b</sup>. The Nataf transformation occurs in the following two steps. To transform between the original correlated x-space variables and correlated standard normals (“z-space”), a CDF matching condition is applied for each of the marginal distributions:

$$\Phi(z_i) = F(x_i) \quad (7)$$

where  $\Phi()$  is the standard normal cumulative distribution function and  $F()$  is the cumulative distribution function of the original probability distribution. Then, to transform between correlated z-space variables and uncorrelated u-space variables, the Cholesky factor  $\mathbf{L}$  of a modified correlation matrix is used:

$$\mathbf{z} = \mathbf{L}\mathbf{u} \quad (8)$$

where the original correlation matrix for non-normals in x-space has been modified to represent the corresponding correlation in z-space.<sup>8</sup>

## III. Non-intrusive polynomial chaos

### A. Galerkin projection

The Galerkin projection approach projects the response against each basis function using inner products and employs the polynomial orthogonality properties to extract each coefficient. From Eq. 5, it is evident that

$$\alpha_j = \frac{\langle R, \Psi_j \rangle}{\langle \Psi_j^2 \rangle} = \frac{1}{\langle \Psi_j^2 \rangle} \int_{\Omega} R \Psi_j \varrho(\boldsymbol{\xi}) d\boldsymbol{\xi}, \quad (9)$$

<sup>b</sup>If joint distributions are known, then the Rosenblatt transformation is preferred.

where each inner product involves a multidimensional integral over the support range of the weighting function. In particular,  $\Omega = \Omega_1 \otimes \cdots \otimes \Omega_n$ , with possibly unbounded intervals  $\Omega_j \subset \mathbb{R}$  and the tensor product form  $\varrho(\boldsymbol{\xi}) = \prod_{i=1}^n \varrho_i(\xi_i)$  of the joint probability density (weight) function. The denominator in Eq. 9 is the norm squared of the multivariate orthogonal polynomial, which can be computed analytically using the product of univariate norms squared

$$\langle \Psi_j^2 \rangle = \prod_{i=1}^n \langle \psi_{m_i^j}^2 \rangle \quad (10)$$

where the univariate inner products have simple closed form expressions for each polynomial in the Askey scheme.<sup>4</sup> Thus, the primary computational effort resides in evaluating the numerator, which is evaluated numerically using either quadrature or sampling approaches.

### 1. Sampling

In the sampling approach, the integral evaluation is equivalent to computing the expectation (mean) of the response-basis function product (the numerator in Eq. 9) for each term in the expansion when sampling within the density of the weighting function.

In computational practice, coefficient estimations based on sampling benefit from first estimating the response mean (the first PCE coefficient) and then removing the mean from the expectation evaluations for all subsequent coefficients.<sup>13</sup> While this has no effect for quadrature methods (see Section III.A.2 below) and little effect for fully-resolved sampling, it does have a small but noticeable beneficial effect for under-resolved sampling.

### 2. Tensor product quadrature

In quadrature-based approaches, the simplest general technique for approximating multidimensional integrals, as in Eq. 9, is to employ a tensor product of one-dimensional quadrature rules. In the case where  $\Omega$  is a hypercube, i.e.  $\Omega = [-1, 1]^n$ , there are several choices of nested abscissas, included Clenshaw-Curtis, Gauss-Patterson, etc.<sup>14–16</sup> In the more general case, we propose to use Gaussian abscissas, i.e. the zeros of the orthogonal polynomials with respect to some positive weight, e.g. Gauss-Hermite, Gauss-Legendre, Gauss-Laguerre, generalized Gauss-Laguerre, or Gauss-Jacobi.

In this section we begin by recalling tensor product quadrature. We first introduce an index  $i \in \mathbb{N}_+$ ,  $i \geq 1$ . Then, for each value of  $i$ , let  $\{y_1^i, \dots, y_{m_i}^i\} \subset \Omega_i$  be a sequence of abscissas for quadrature on  $\Omega_i$ .

For  $f \in C^0(\Omega_i)$  and  $n = 1$  we introduce a sequence of one-dimensional quadrature operators

$$\mathcal{Q}^i(f)(\xi) = \sum_{j=1}^{m_i} u(\xi_j^i) w_j^i, \quad (11)$$

with  $m_i \in \mathbb{N}$  given. When utilizing Gaussian quadrature, Eq. 11 integrates exactly all polynomials of degree less than  $2m_i - 1$ , for each  $i = 1, \dots, n$ . Given an expansion order  $p$ , the highest order coefficient evaluations (Eq. 9) can be assumed to involve integrands of at least polynomial order  $2p$  ( $\Psi$  of order  $p$  and  $R$  modeled to order  $p$ ) in each dimension such that a minimal Gaussian quadrature order of  $p + 1$  will be required to obtain good accuracy in these coefficients.

Now, in the multivariate case  $n > 1$ , for each  $u \in C^0(\Omega)$  and the multi-index  $\mathbf{i} = (i_1, \dots, i_n) \in \mathbb{N}_+^n$  we define the full tensor product quadrature formulas

$$\mathcal{Q}_{\mathbf{i}}^n u(y) = (\mathcal{Q}^{i_1} \otimes \cdots \otimes \mathcal{Q}^{i_n})(f)(\boldsymbol{\xi}) = \sum_{j_1=1}^{m_{i_1}} \cdots \sum_{j_n=1}^{m_{i_n}} f(\xi_{j_1}^{i_1}, \dots, \xi_{j_n}^{i_n}) (w_{j_1}^{i_1} \otimes \cdots \otimes w_{j_n}^{i_n}). \quad (12)$$

Clearly, the above product needs  $\prod_{j=1}^n m_{i_j}$  function evaluations. Therefore, when the number of input random variables is small, full tensor product quadrature is a very effective numerical tool. On the other hand, approximations based on tensor product grids suffer from the *curse of dimensionality* since the number of collocation points in a tensor grid grows exponentially fast in the number of input random variables. For example, if Eq. 12 employs the same order for all random dimensions,  $m_{i_j} = m$ , then Eq. 12 requires  $M = m^n$  function evaluations.

### 3. Sparse grid Smolyak cubature

If the number of random variables is moderately large, one should rather consider sparse tensor product spaces as first proposed by Smolyak<sup>17</sup> and further investigated by Refs. 14–16, 18–20 that reduce dramatically the number of collocation points, while preserving a high level of accuracy.

Here we follow the notation and extend the description in Ref. 14 to describe the Smolyak *isotropic* formulas  $\mathcal{A}(w, n)$ . The Smolyak formulas are just linear combinations of the product formulas in Eq. 12 with the following key property: only products with a relatively small number of points are used. With  $\mathcal{U}^0 = 0$  and for  $i \in \mathbb{N}_+$  define

$$\Delta^i := \mathcal{U}^i - \mathcal{U}^{i-1}. \quad (13)$$

Moreover, given an integer  $w \in \mathbb{N}_+$ , hereafter called the *level*, we define the sets

$$X(w, n) := \left\{ \mathbf{i} \in \mathbb{N}_+^n, \mathbf{i} \geq \mathbf{1} : \sum_{k=1}^n (i_k - 1) \leq w \right\}, \quad (14a)$$

$$\tilde{X}(w, n) := \left\{ \mathbf{i} \in \mathbb{N}_+^n, \mathbf{i} \geq \mathbf{1} : \sum_{k=1}^n (i_k - 1) = w \right\}, \quad (14b)$$

$$Y(w, n) := \left\{ \mathbf{i} \in \mathbb{N}_+^n, \mathbf{i} \geq \mathbf{1} : w - n + 1 \leq \sum_{k=1}^n (i_k - 1) \leq w \right\}, \quad (14c)$$

and for  $\mathbf{i} \in \mathbb{N}_+^n$  we set  $|\mathbf{i}| = i_1 + \dots + i_n$ . Then the isotropic Smolyak quadrature formula is given by

$$\mathcal{A}(w, n) = \sum_{\mathbf{i} \in X(w, n)} (\Delta^{i_1} \otimes \dots \otimes \Delta^{i_n}). \quad (15)$$

Equivalently, formula Eq. 15 can be written as<sup>21</sup>

$$\mathcal{A}(w, n) = \sum_{\mathbf{i} \in Y(w, n)} (-1)^{w+n-|\mathbf{i}|} \binom{n-1}{w+n-|\mathbf{i}|} \cdot (\mathcal{U}^{i_1} \otimes \dots \otimes \mathcal{U}^{i_n}). \quad (16)$$

To compute  $\mathcal{A}(w, n)(f)$ , one only needs to know function values on the “sparse grid”

$$\mathcal{H}(w, n) = \bigcup_{\mathbf{i} \in Y(w, n)} (\vartheta^{i_1} \times \dots \times \vartheta^{i_n}) \subset \Omega, \quad (17)$$

where  $\vartheta^i = \{y_1^i, \dots, y_{m_i}^i\} \subset \Omega_i$  denotes the set of abscissas used by  $\mathcal{U}^i$ . If the sets are nested, i.e.  $\vartheta^i \subset \vartheta^{i+1}$ , then  $\mathcal{H}(w, n) \subset \mathcal{H}(w+1, n)$  and

$$\mathcal{H}(w, n) = \bigcup_{\mathbf{i} \in \tilde{X}(w, n)} (\vartheta^{i_1} \times \dots \times \vartheta^{i_n}). \quad (18)$$

By comparing Eq. 18 and Eq. 17, we observe that the Smolyak approximation that employs nested points requires less function evaluations than the corresponding formula with non-nested points.

Examples of isotropic sparse grids, constructed from the nested Clenshaw-Curtis abscissas and the non-nested Gaussian abscissas are shown in Figure 1, where  $\Omega = [-1, 1]^2$ . There, we consider a two-dimensional parameter space and a maximum level  $w = 5$  (sparse grid  $\mathcal{H}(5, 2)$ ). To see the reduction in function evaluations with respect to full tensor product grids, we also include a plot of the corresponding Clenshaw-Curtis isotropic full tensor grid having the same maximum number of points in each direction, namely  $2^w + 1 = 33$ .

Note that the Smolyak approximation formula, as presented in this Section, is isotropic, since all directions are treated equally. This can be seen from Eq. 15 observing that if a multi-index  $\mathbf{i} = (i_1, i_2, \dots, i_n)$  belongs to the set  $X(w, n)$ , then any permutation of  $\mathbf{i}$  also belongs to  $X(w, n)$  and contributes to the construction of the Smolyak approximation  $\mathcal{A}(w, n)$ . Observe that if we take  $m$  points in each direction, the isotropic full tensor grid will contain  $m^n$  points while the analogous isotropic Smolyak grid  $\mathcal{H}(w, n)$  will contain much less points. Figure 2 shows the total number of points contained in the full tensor grid and in the Smolyak sparse

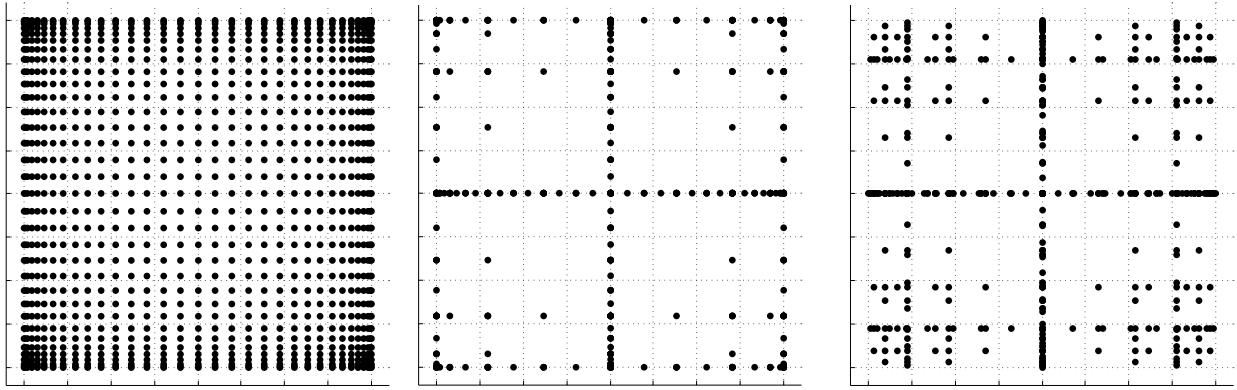


Figure 1. For a two-dimensional parameter space ( $N = 2$ ) and maximum level  $w = 5$ , we plot the full tensor product grid using the Clenshaw-Curtis abscissas (left) and isotropic Smolyak sparse grids  $\mathcal{H}(5, 2)$ , utilizing the Clenshaw-Curtis abscissas (middle) and the Gaussian abscissas (right).

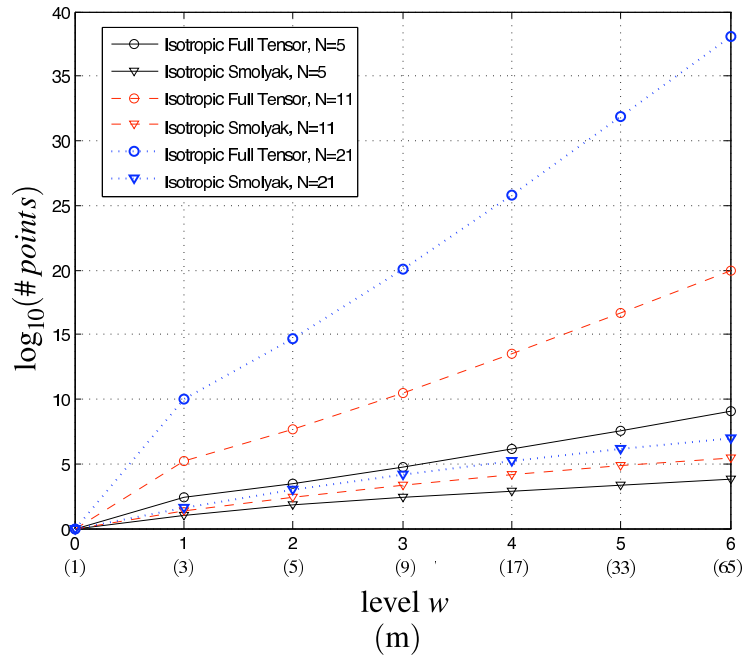


Figure 2. For a finite dimensional  $\Gamma^N$  with  $N = 5, 11$  and  $21$  we plot the log of the number of distinct Clenshaw-Curtis points used by the isotropic Smolyak method and the corresponding isotropic full tensor product method versus the level  $w$  (or the maximum number of points  $m$  employed in each direction).

grid as a function of the level  $w$  (or the corresponding maximum number  $m$  of points in each direction), for dimensions  $n = 5, 11, 21$ .

To exhibit the efficiency of the *isotropic* sparse grid method we briefly compare its convergence with *isotropic* tensor product methods. For more details, see Ref. 14. An isotropic full tensor product quadrature method converges roughly like  $C(\sigma, n)M^{-\sigma/N}$ , where  $\sigma$  is related to the smoothness of the integrand and  $M$  is the total number of samples. The slowdown effect that the dimension  $N$  has on the last convergence is known as the curse of dimensionality and it is the reason for not using isotropic full tensor quadrature for large values of  $N$ . On the other hand, the isotropic Smolyak approximation seems to be better suited for this case. Indeed, in Ref. 14 it was shown that the convergence of the Smolyak techniques has a much faster exponent  $\mathcal{O}(\frac{\sigma}{\log(2N)})$ . This is a clear advantage of the isotropic Smolyak method with respect to the

full tensor and justifies how the Smolyak approximation greatly reduces the curse of dimensionality.

Furthermore, Ref. 14 revealed that the isotropic Smolyak algorithm is effective for problems whose input data depend on a moderate number of random variables, which “weigh equally” in the solution. For such isotropic situations the displayed convergence is faster than standard quadrature techniques built upon full tensor product spaces. On the other hand, the convergence rate of the sparse grid algorithm deteriorates for highly anisotropic problems, such as those appearing when the input random variables come e.g. from Karhunen-Loève -type truncations of “smooth” random fields. In such cases, a full anisotropic tensor product approximation<sup>22,23</sup> may still be more effective for a small or modest number of random variables. However, if the number of random variables is large, anisotropic Smolyak cubature methods have been developed which exhibit improved scaling with problem size.<sup>15</sup> Since most of these anisotropic ideas have been developed in the context of Stochastic Collocation we will not explore these methods in this paper as we are continuing to extend them for the polynomial chaos setting.

## B. Linear regression

The linear regression approach (also known as point collocation or stochastic response surfaces<sup>24,25</sup>) uses a single linear least squares solution of the form:

$$\Psi \alpha = R \quad (19)$$

to solve for the complete set of PCE coefficients  $\alpha$  that best match a set of response values  $R$ . The set of response values is typically obtained by performing a design of computer experiments within the density function of  $\xi$ , where each row of the matrix  $\Psi$  contains the  $N$  multivariate polynomial terms  $\Psi_j$  evaluated at a particular  $\xi$  sample. An over-sampling is generally advisable (Ref. 25 recommends  $2N$  samples), resulting in a least squares solution for the over-determined system. In the case of  $2N$  oversampling, the simulation requirements for this approach scale as  $\frac{2(n+p)!}{n!p!}$ , which can be significantly more affordable than isotropic tensor-product quadrature (e.g.,  $(p+1)^n$ ) for larger problems.

## IV. Computational Results

Wiener-Askey generalized polynomial chaos has been implemented in DAKOTA,<sup>26</sup> an open-source software framework for design and performance analysis of computational models on high performance computers. This section presents PCE performance results for several algebraic benchmark test problems and an elliptic PDE problem. PCE-based optimization under uncertainty computational experiments and results are presented in Ref. 27.

### A. Lognormal ratio

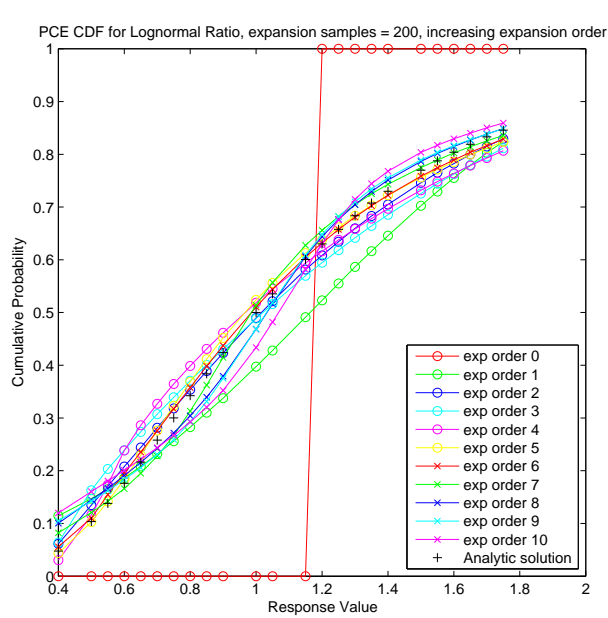
This test problem has a limit state function (i.e., a critical response metric which defines the boundary between safe and failed regions of the random variable parameter space) defined by the ratio of two correlated, identically-distributed random variables.

$$g(\mathbf{x}) = \frac{x_1}{x_2} \quad (20)$$

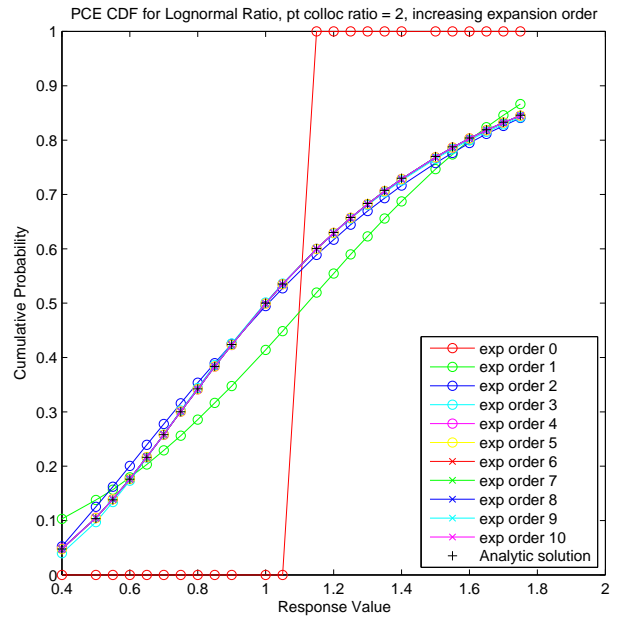
The distributions for both  $x_1$  and  $x_2$  are Lognormal(1, 0.5) with a correlation coefficient between the two variables of 0.3. Hermite chaos is used based on the close relationship between lognormal and normal random variables.

For the UQ analysis, 24 response levels (.4, .5, .55, .6, .65, .7, .75, .8, .85, .9, 1, 1.05, 1.15, 1.2, 1.25, 1.3, 1.35, 1.4, 1.5, 1.55, 1.6, 1.65, 1.7, and 1.75) are mapped into the corresponding cumulative probability levels. For this problem, an analytic solution is available and is used for comparison to CDFs generated from sampling on the chaos expansions using  $10^5$  samples. Figure 3 shows computational results for increasing expansion orders for each of the coefficient estimation approaches.

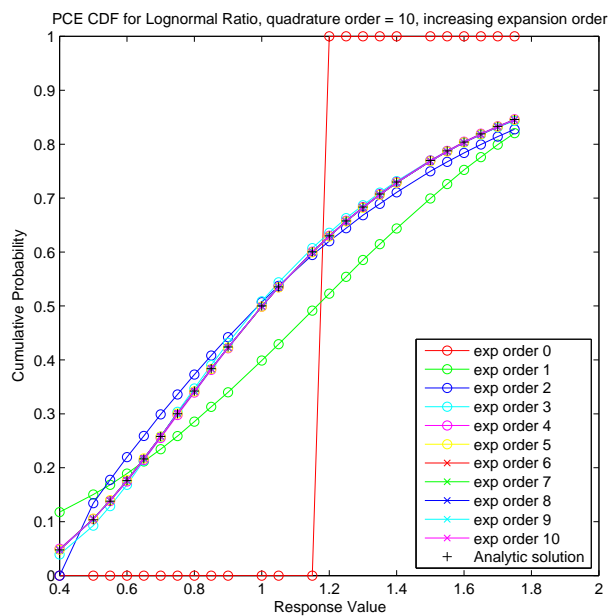
In Figure 3(a), it is evident that 200 expansion samples (approach from Section III.A.1) are insufficient to allow convergence in the higher order PCE coefficients, such that the higher order expansions can actually be less accurate than the lower order expansions. In Figures 3(b,c,d), superior convergence behavior is observed when using point collocation (Section III.B), tensor-product Gaussian quadrature (Section III.A.2), and sparse-grid Gaussian cubature (Section III.A.3) approaches. The number of simulations is fixed at two times



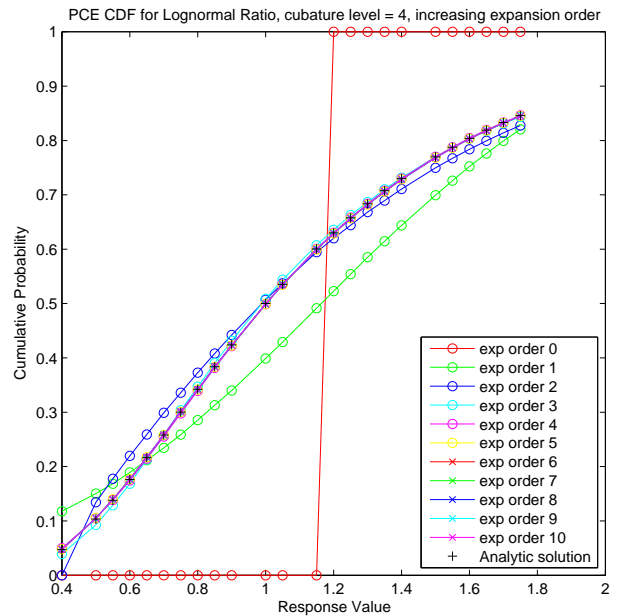
(a) Expansion samples = 200.



(b) Point collocation ratio = 2.



(c) Quadrature order = 10.



(d) Cubature level = 4.

Figure 3. Convergence of PCE for increasing expansion orders for lognormal ratio test problem.

the number of expansion terms (2, 6, 12, 20, 30, 42, 56, 72, 90, 110, and 132 simulations for expansion orders 0–10) in the point collocation case, at  $10^{th}$  order quadrature ( $10^2$  simulations for 2 variables) in the quadrature case, and at cubature level = 4 (221 simulations) for the sparse grid case. In each of these three cases, the CDFs are visually indistinguishable by fourth order.

In Figure 4, CDF residuals are plotted for quadrature, point collocation, and sampling on a log-linear graph as a function of increasing expansion order. It is worth highlighting that this breaks with the common convention of plotting convergence in the first two moments, instead focusing on the full CDF (including tails). It is evident that improvement stalls for the 200 expansion samples case following the second order expansion. Improvement continues with a linear convergence rate with respect to expansion order for the quadrature and point collocation approaches and appears to primarily be limited by the resolution of the sample set used to evaluate the PCE. Cubature results (not shown) are essentially identical to the quadrature results for this plot.

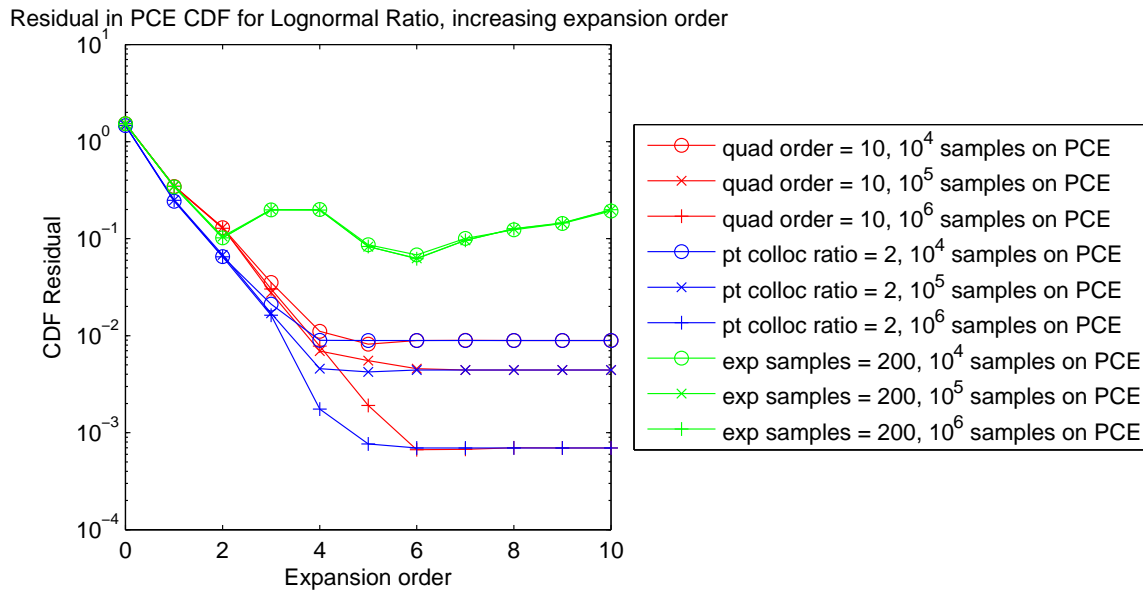


Figure 4. Log-linear convergence of PCE for increasing expansion orders for lognormal ratio test problem.

In Figure 5, CDF residuals are plotted for each of the coefficient estimation approaches on a log-log graph as a function of increasing simulation evaluations. For the quadrature approach, the expansion order  $p$  is varied from 0 to 10, with the quadrature order set at  $p + 1$ . For the cubature approach, the cubature level  $w$  is varied from 0 to 4, with the expansion order  $p$  set based on  $2p \leq m$  for  $m = 2^{w+1} - 1$ . For the point collocation approach, the expansion order is varied from 0 to 10 with the over-sampling ratio set at 2. And for the sampling approach, the expansion order is fixed at 10 and the expansion samples are varied between 1 and  $10^5$  by orders of 10. It is evident that the convergence rates for quadrature, cubature, and point collocation are super-algebraic/exponential in nature with respect to simulation evaluations, whereas the convergence rate for sampling is algebraic with the expected slope of  $\frac{1}{2}$  (sample estimates converge as the square root of the number of samples). From these results, it can be concluded that Hermite chaos is also an excellent basis choice for lognormal random variables, which should not be surprising given the exact analytic transformation from (correlated) lognormals in  $x$ -space to uncorrelated standard normals in  $u$ -space (where the chaos expansion is applied). This analytic relationship is stronger than one based only on CDF equivalence. From this, it can be inferred that Legendre chaos would also be an excellent choice for loguniform distributions.

## B. Rosenbrock

The Rosenbrock function is a popular test problem for gradient-based optimization algorithms due to its difficulty for first-order methods. It turns out that this is also a challenging problem for certain UQ methods (especially local reliability methods), since a particular response level contour involves a highly nonlinear

Residual in PCE CDF for Lognormal Ratio, increasing simulations

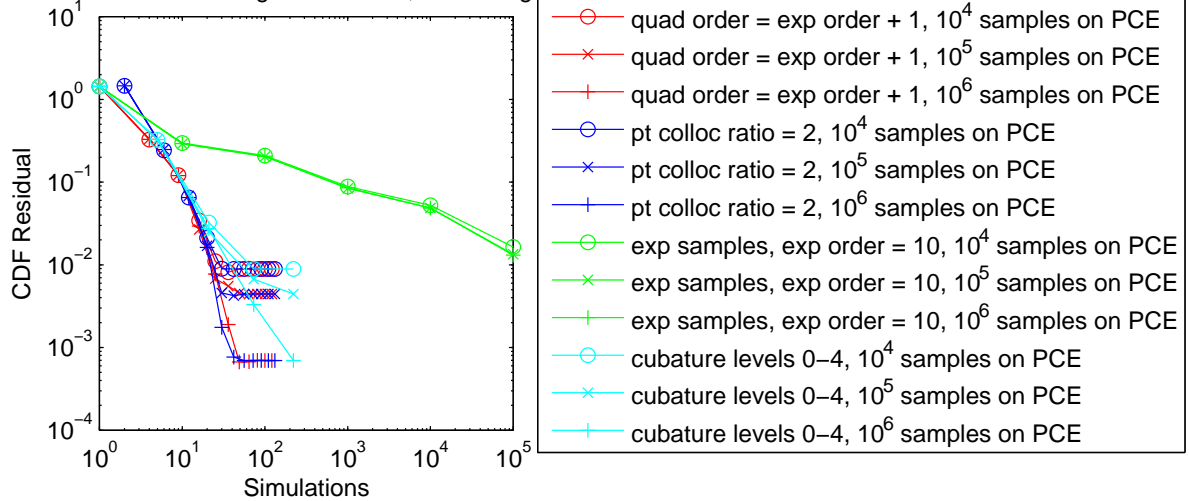


Figure 5. Log-log convergence of PCE for increasing simulation evaluations for lognormal ratio test problem.

curve that encircles the mean point. The two-variable version of this function is a fourth order polynomial of the form:

$$f(x_1, x_2) = 100(x_2 - x_1^2)^2 + (1 - x_1)^2 \tag{21}$$

A three-dimensional plot of this function is shown in Figure 6(a), where both  $x_1$  and  $x_2$  range in value from -2 to 2. Figure 6(b) shows a contour plot for Rosenbrock’s function, demonstrating the encircling of the mean.

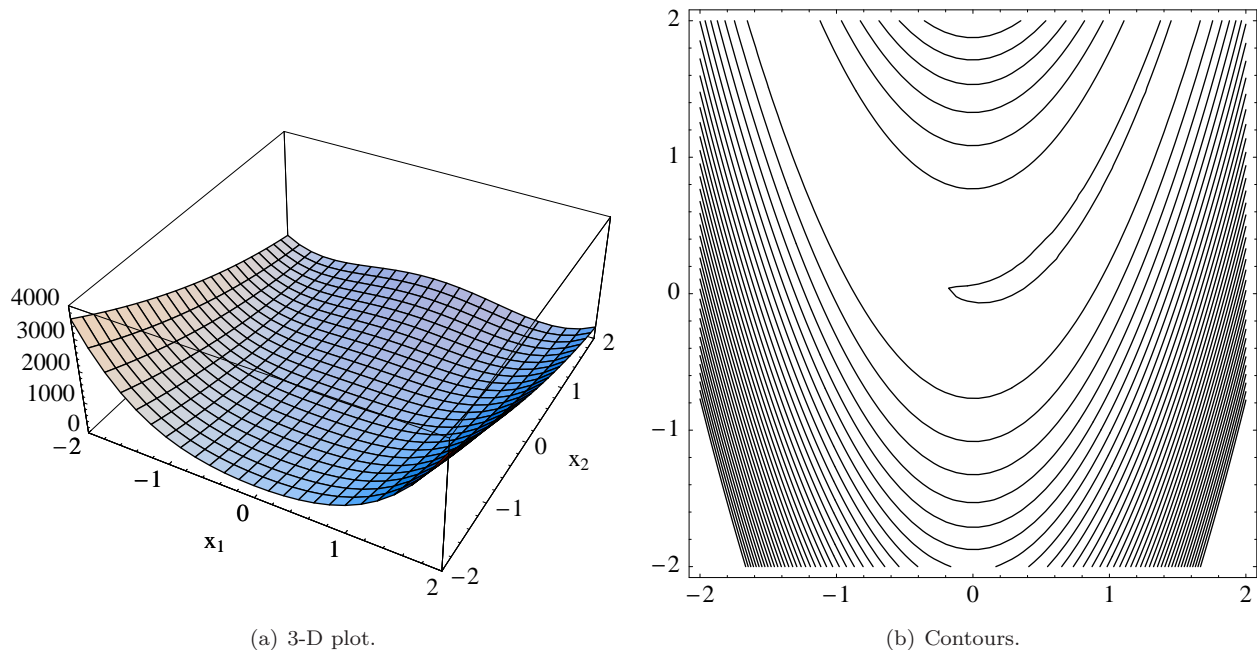


Figure 6. Rosenbrock’s function.

For the UQ analysis,  $x_1$  and  $x_2$  are modeled as uncorrelated standard normals ( $N(0,1)$ ,  $\rho_{12} = 0$ .) and six response levels (.1, 1., 50., 100., 500., and 1000.) are mapped into the corresponding cumulative probability levels. Hermite chaos is used and would be expected to demonstrate optimal convergence for these variables. Since analytic CDF solutions are not available for this problem or any of the test problems to follow,

accuracy comparisons involve comparisons of statistics generated by sampling on the PCE approximation with statistics generated by sampling on the original response metric, where the sampling sets are of the same size and generated with the same random seed. The only difference in the sample sets is that the PCE samples are generated based on  $\xi$  (independent distributions in standard form) whereas the original response samples are generated based on  $\mathbf{x}$  (correlated distributions in original form), such that minor discrepancies could be introduced in cases where the transformations (Eqs. 7-8) are not exact (e.g., some correlation warping expressions from Ref. 8). Outside of this case, however, it can be inferred that the PCE captures the input/output relationship highly accurately, and in some cases exactly, when there is no detectable difference in the sample-generated CDFs. Computational results demonstrating these types of comparisons are shown for increasing expansion orders in Figure 7 and for fixed expansion order in Figure 8.

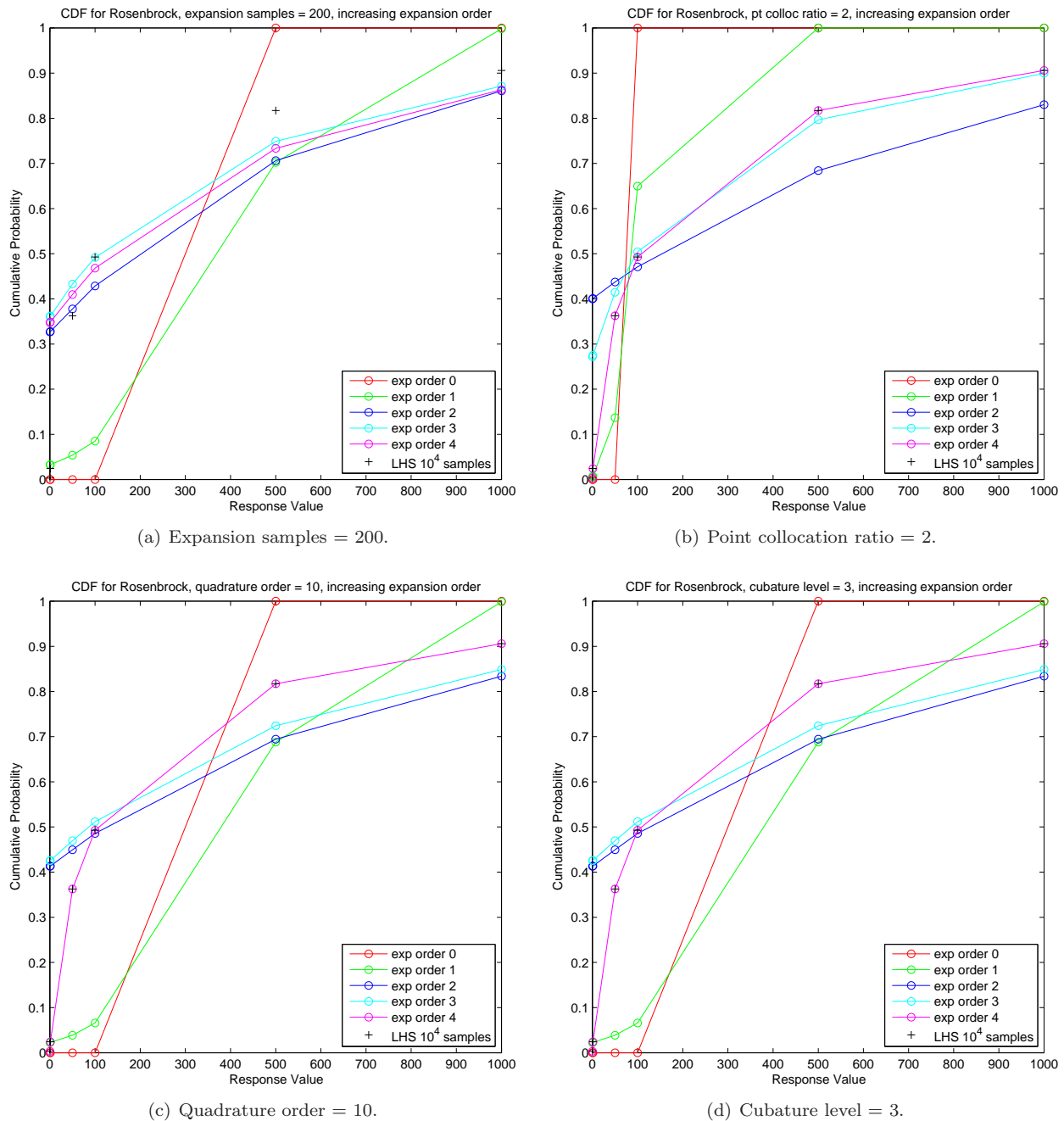


Figure 7. Convergence of PCE for increasing expansion orders for Rosenbrock test problem.

In Figure 7(a), it is evident that 200 expansion samples again do a poor job in converging the PCE coefficients and order convergence to the LHS result is not obtained. In Figures 7(b,c,d), superior convergence behavior is again observed when using point collocation (simulations equal to two times the number of expansion terms), Gaussian quadrature ( $10^{\text{th}}$  order quadrature using  $10^2$  simulations), and Gaussian cubature (level = 3 using 73 simulations) approaches. In each of these three cases, the expansion is exact by fourth order, as would be expected in this problem (a fourth order polynomial function of normal variates). Increasing the expansion order beyond four has no effect as all higher-order coefficients are calculated to be less than  $10^{-15}$ .

In Figure 8, the expansion order has been fixed at four, since it is known that higher order expansion terms do not contribute for this problem. In Figure 8(a), the number of expansion samples is increased to assess the convergence rate to the exact expansion coefficients. It is evident that the rate is unacceptably slow, with the PCE coefficients resulting from  $10^6$  simulations still not producing the accuracy of a fifth order isotropic quadrature (25 simulations). In Figure 8(b), the exact coefficients are obtained for a quadrature order of five or greater, as expected for integrals (Eq. 9) involving a product of a fourth order function and fourth order expansion terms (refer to Section III.A.2). Thus with *a priori* knowledge of the order of the problem (or a smart adaptive technique), excellent accuracy can be obtained using a fourth order chaos expansion and fifth order quadrature, at the expense of only 25 simulations. Furthermore, with anisotropic integration tailoring, the expansion can be integrated exactly with fifth order quadrature in  $x_1$  and fourth order quadrature in  $x_2$ , reducing the expense to 20 simulations. Cubature results in Figure 8(c) are exact by level three, at an expense of 73 simulations, demonstrating that quadrature can outperform cubature for low dimensional problems.

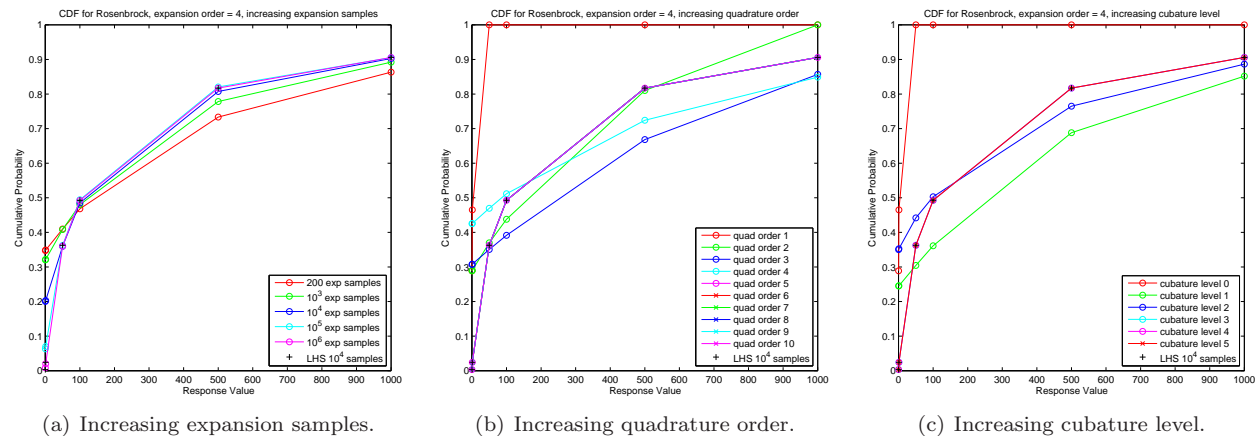


Figure 8. Convergence of PCE for fixed expansion order = 4 for Rosenbrock test problem.

In Figure 9, the expansion order is again fixed at four, and we vary the distribution type and polynomial basis, including two standard normal variables using a Hermite basis, two uniform variables on  $[-2, 2]$  using a Legendre basis, two exponential variables with  $\beta = 2$  using a Laguerre basis, two beta variables with  $\alpha = 1$  and  $\beta = 0.5$  using a Jacobi basis, two gamma variables with  $\alpha = 1.5$  and  $\beta = 2$  using a generalized Laguerre basis, and five variables (normal, uniform, exponential, beta, and gamma with the same distribution parameters) using a mixed basis. For the mixed expansion over five variables, the standard two-dimensional Rosenbrock is generalized to n-dimensions as defined in Ref. 28. In each case, fifth-order tensor product quadrature is used (25 evaluations each for Hermite, Legendre, Laguerre, Jacobi, and generalized Laguerre cases, and 3125 evaluations for the mixed case). For point collocation with an oversampling ratio of two, the same results can be generated using 30 evaluations for Hermite, Legendre, Laguerre, Jacobi, and generalized Laguerre cases and only 252 evaluations for the five variable mixed case. In all cases, the expansion is exact as expected, which provides verification of the Askey basis implementation.

### C. Short column

This test problem involves the plastic analysis of a short column with rectangular cross section (width  $b = 5$  and depth  $h = 15$ ) having uncertain material properties (yield stress  $Y$ ) and subject to uncertain loads (bending moment  $M$  and axial force  $P$ ).<sup>29</sup> The limit state function is defined as:

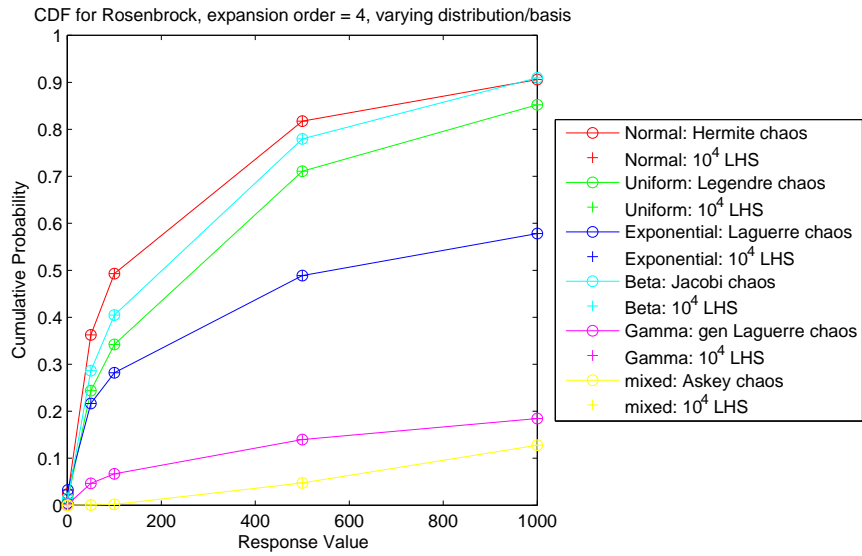


Figure 9. Varying distribution type and PCE basis for Rosenbrock test problem with fixed expansion order = 4 and fixed quadrature order = 5.

$$g(\mathbf{x}) = 1 - \frac{4M}{bh^2Y} - \frac{P^2}{b^2h^2Y^2} \quad (22)$$

The distributions for  $P$ ,  $M$ , and  $Y$  are Normal(500, 100), Normal(2000, 400), and Lognormal(5, 0.5), respectively, with a correlation coefficient of 0.5 between  $P$  and  $M$  (uncorrelated otherwise). 43 response levels (-9.0, -8.75, -8.5, -8.0, -7.75, -7.5, -7.25, -7.0, -6.5, -6.0, -5.5, -5.0, -4.5, -4.0, -3.5, -3.0, -2.5, -2.0, -1.9, -1.8, -1.7, -1.6, -1.5, -1.4, -1.3, -1.2, -1.1, -1.0, -0.9, -0.8, -0.7, -0.6, -0.5, -0.4, -0.3, -0.2, -0.1, 0.0, 0.05, 0.1, 0.15, 0.2, 0.25) are mapped into the corresponding cumulative probability levels. Computational results are shown in Figure 10 for increasing expansion orders of Hermite chaos, where tensor-product Gaussian quadrature is used in each case with quadrature order set to  $p + 1$ . Results generated from sampling on the expansion are compared to a set of reference results generated from sampling on the original limit state. By expansion order = 2 (at an expense of 27 simulations), the CDF shape has been captured (Figure 10(a)), and by expansion order = 4 (at an expense of 125 simulations), the statistics are converged in the extreme tails (Figures 10(b,c)). Alternatively, point collocation generates similar results using 20 simulations for  $p = 2$  and 70 simulations for  $p = 4$ , and Gaussian cubature generates similar results for both orders using 159 simulations (cubature level = 3).

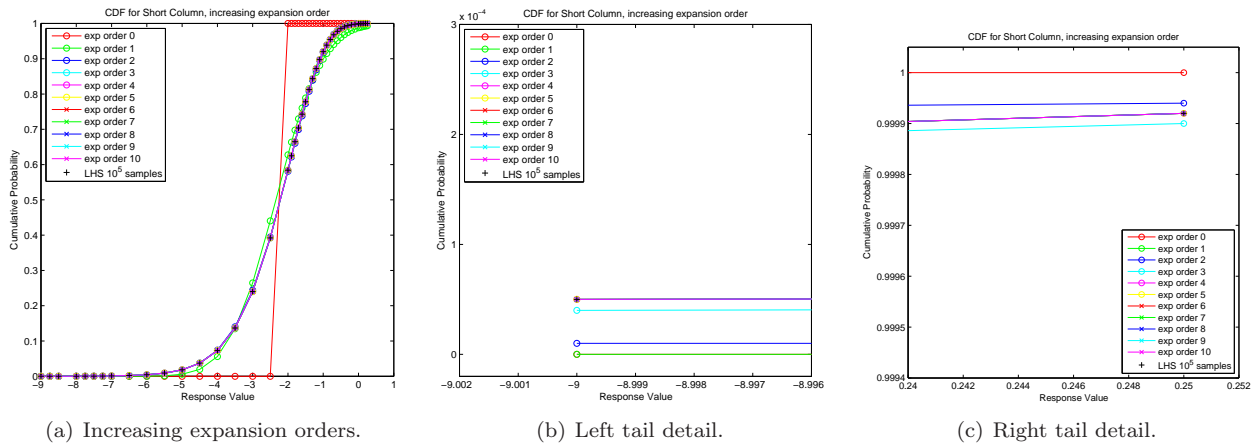


Figure 10. Convergence of PCE for increasing expansion orders for short column test problem.

## D. Cantilever beam

The next test problem involves the simple uniform cantilever beam<sup>30,31</sup> shown in Figure 11.

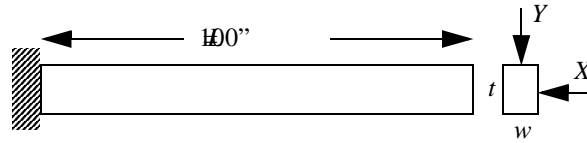


Figure 11. Cantilever beam test problem.

Random variables in the problem include the yield stress  $R$  and Youngs modulus  $E$  of the beam material and the horizontal and vertical loads,  $X$  and  $Y$ , which are modeled with normal distributions using  $N(40000, 2000)$ ,  $N(2.9E7, 1.45E6)$ ,  $N(500, 100)$ , and  $N(1000, 100)$ , respectively. Problem constants include  $L = 100$  in. and  $D_0 = 2.2535$  in. The beam response metrics have the following analytic form:

$$\text{stress} = \frac{600}{wt^2}Y + \frac{600}{w^2t}X \leq R \quad (23)$$

$$\text{displacement} = \frac{4L^3}{Ewt} \sqrt{\left(\frac{Y}{t^2}\right)^2 + \left(\frac{X}{w^2}\right)^2} \leq D_0 \quad (24)$$

When formulated as scaled optimization constraints ( $\frac{\text{stress}}{R} - 1$  and  $\frac{\text{displacement}}{D_0} - 1$ , where negative values are feasible), 11 response levels (0.0 to 1.0 in 0.1 increments) are mapped into the corresponding cumulative probability levels for each function. Computational results are shown in Figures 12 and 13 for increasing expansion orders of Hermite chaos, where tensor-product Gaussian quadrature is used in each case with quadrature order set to  $p + 1$ . For both metrics, the basic CDF shape has been captured using only a

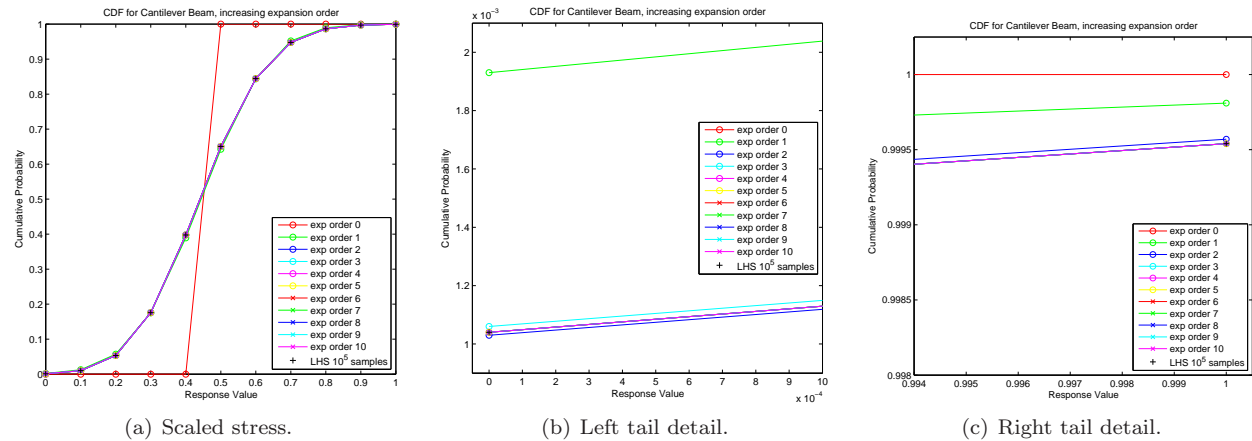


Figure 12. Convergence of PCE for increasing expansion orders for scaled stress metric in cantilever beam test problem.

first-order expansion (Figures 12(a) and 13(a)) at an expense of only 16 simulations (10 for point collocation, 9 for cubature with level = 1), and the statistics are converged in the tails (Figures 12(b,c) and 13(b,c)) by third- or fourth-order expansions at an expense of 256 or 625 simulations, respectively (70 or 140 for point collocation, 289 for cubature with level = 3).

## E. Steel Column

The final test problem involves the trade-off between cost and reliability for a steel column.<sup>29</sup> The cost is defined as

$$\text{Cost} = bd + 5h \quad (25)$$

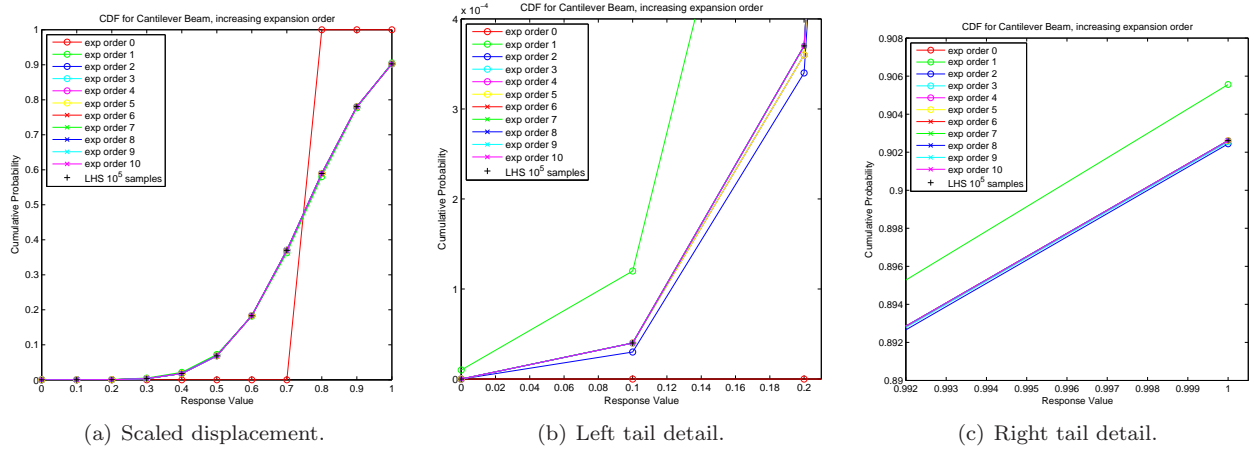


**Figure 13. Convergence of PCE for increasing expansion orders for scaled displacement metric in cantilever beam test problem.**

where  $b$ ,  $d$ , and  $h$  are the means of the flange breadth, flange thickness, and profile height, respectively. This problem demonstrates the efficiency of different coefficient estimation approaches when scaled to larger dimensional UQ problems. Nine uncorrelated random variables are used in the problem to define the yield stress  $F_s$  (lognormal with  $\mu/\sigma = 400/35$  MPa), dead weight load  $P_1$  (normal with  $\mu/\sigma = 500000/50000$  N), variable load  $P_2$  (gumbel with  $\mu/\sigma = 600000/90000$  N), variable load  $P_3$  (gumbel with  $\mu/\sigma = 600000/90000$  N), flange breadth  $B$  (lognormal with  $\mu/\sigma = b/3$  mm), flange thickness  $D$  (lognormal with  $\mu/\sigma = d/2$  mm), profile height  $H$  (lognormal with  $\mu/\sigma = h/5$  mm), initial deflection  $F_0$  (normal with  $\mu/\sigma = 30/10$  mm), and Youngs modulus  $E$  (weibull with  $\mu/\sigma = 21000/4200$  MPa). The limit state has the following analytic form:

$$g = F_s - P \left( \frac{1}{2BD} + \frac{F_0}{BDH} \frac{E_b}{E_b - P} \right) \quad (26)$$

where

$$P = P_1 + P_2 + P_3 \quad (27)$$

$$E_b = \frac{\pi^2 EBDH^2}{2L^2} \quad (28)$$

and the column length  $L$  is 7500 mm. Computational results are shown in Figure 14 for increasing expansion orders of Hermite chaos, where 21 response levels (-500 to 1500 in 100 increments) are mapped into the corresponding cumulative probability levels and  $(b, d, h)$  are fixed at (300, 20, 300). Since this problem contains extreme value distributions (gumbel and weibull) which lack an optimal Askey basis, convergence can be expected to be suboptimal, and it is evident that the CDF is not converging. In fact, the variance is diverging (see standard deviation in Figure 14(c)), resulting in more slowly varying CDFs as the expansion order is increased. Figures 15 and 16 show similar results for tensor-product Gaussian quadrature with quadrature order set to  $p + 1$  and for sparse grid Gaussian cubature with level fixed at three. While the quadrature results appear to be the best of the three, only the lowest order quadrature solutions were computationally tractable and it is evident in all cases that the variance is diverging.

To determine whether this convergence difficulty stems from the use of non-optimal bases or some other issue (e.g., a singularity resulting from subtractive cancellation in the denominator of Eq. 26), the steel column problem may be modified to replace the gumbel and weibull extreme value distributions with normal distributions (using the same means and standard deviations reported above) such that only normal and lognormal distributions are present. Figure 17 shows results for this modified problem for increasing expansion orders and a modified set of response levels. It is evident that convergence is rapid in this case and the expansion is accurate by first order. In addition, an LHS convergence study run to  $10^6$  samples for the original, unmodified problem did not demonstrate any divergence in variance, so evidence for a singularity is currently lacking. Rather, the use of Hermite bases for standard normals transformed from extreme value distributions appears to be problematic. Similar difficulties have been observed in Ref. 1 for non-optimal basis selections.

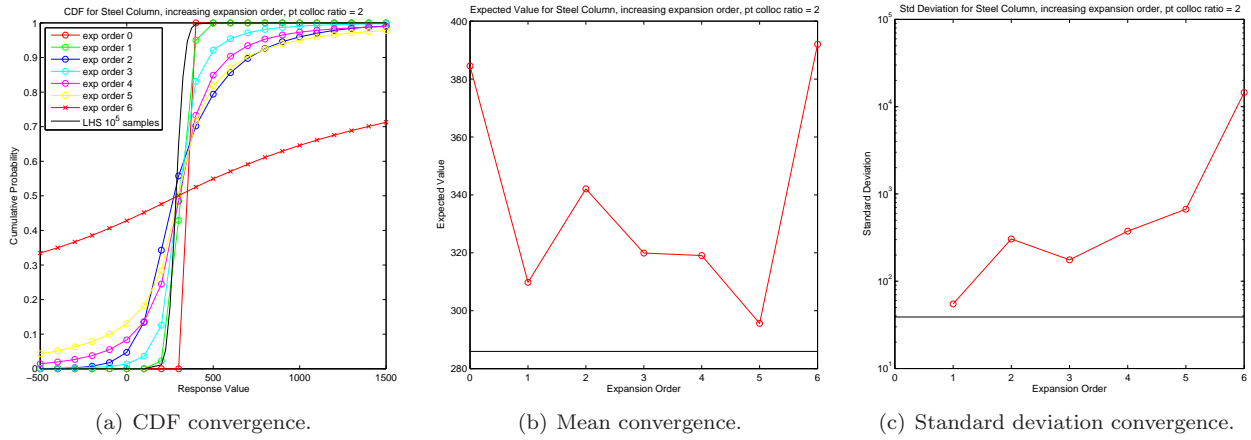


Figure 14. Convergence of PCE for increasing expansion orders for steel column test problem; point collocation ratio = 2.

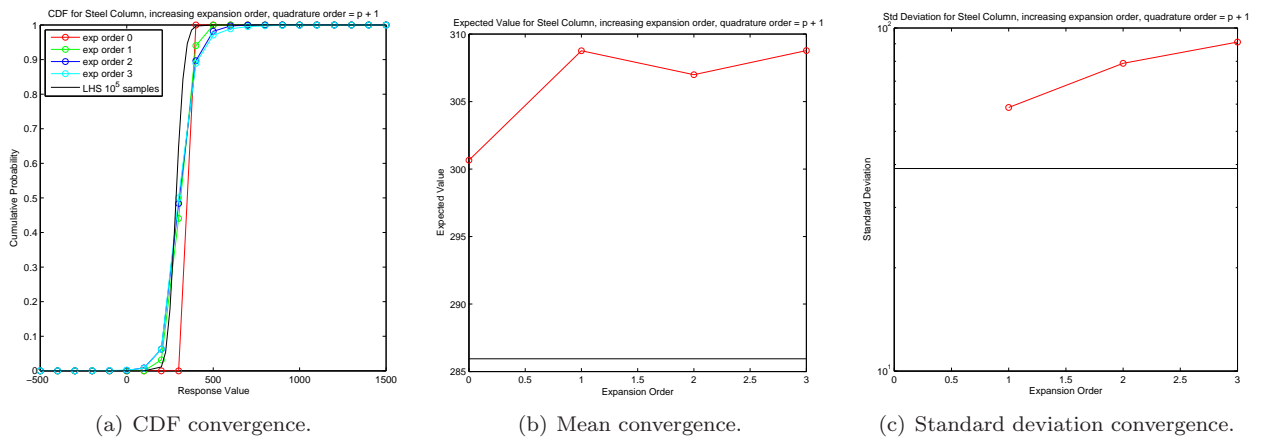


Figure 15. Convergence of PCE for increasing expansion orders for steel column test problem; quadrature order =  $p + 1$ .

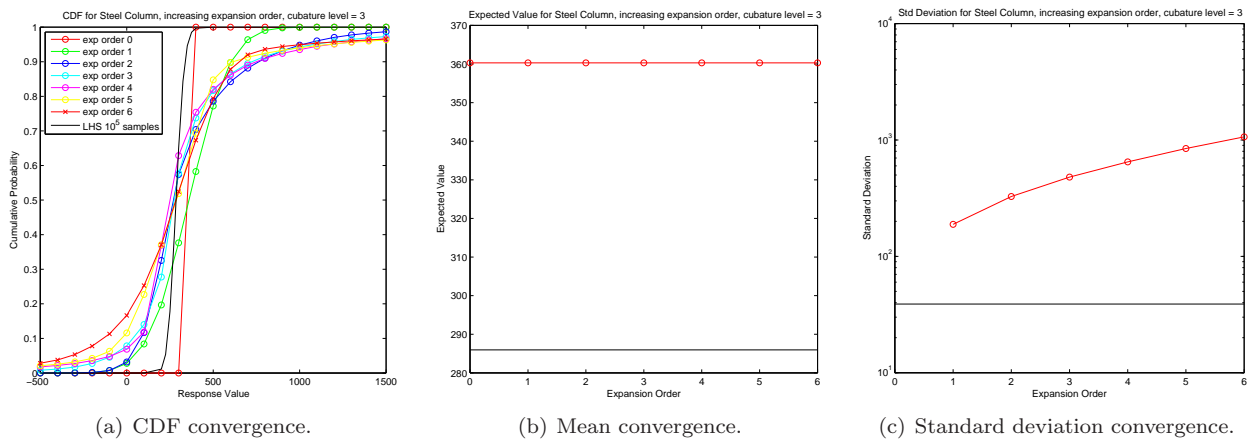


Figure 16. Convergence of PCE for increasing expansion orders for steel column test problem; cubature level = 3.

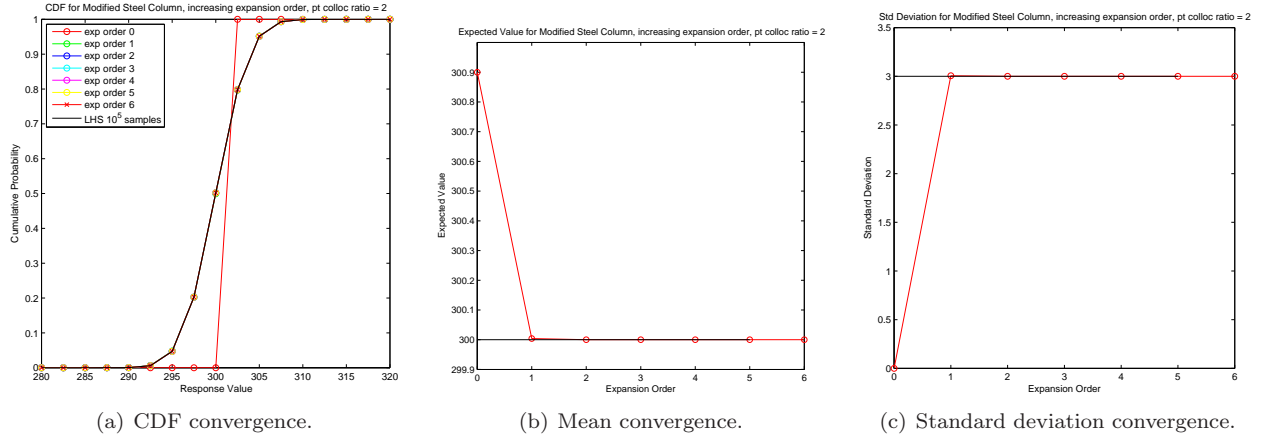


Figure 17. Convergence of PCE for increasing expansion orders for modified steel column test problem; point collocation ratio = 2.

## F. Simulation Requirements

Table 2 summarizes the simulation evaluation requirements of the different algebraic test problems for tensor-product Gaussian quadrature (TP), sparse grid Gaussian cubature (SG), and point collocation (PC), with increasing random variable dimensionality of  $n = 2$  (lognormal ratio, Rosenbrock),  $n = 3$  (short column),  $n = 4$  (cantilever beam),  $n = 5$  (generalized Rosenbrock), and  $n = 9$  (steel column) and chaos expansion order ranging from  $p = 0$  to  $p = 10$ . For all test cases, quadrature and cubature integrations are isotropic and point collocation uses an over-sampling ratio of two. Required cubature levels are approximated, but the approximation is consistent across all problems. It is evident that tensor-product quadrature is the most

Table 2. Simulation evaluation expense for algebraic benchmark test problems.

$p$	Log Ratio/Rosen	Short Column	Cantilever Beam	Gen Rosen	Steel Column
	TP/SG/PC	TP/SG/PC	TP/SG/PC	TP/SG/PC	TP/SG/PC
0	1/1/2	1/1/2	1/1/2	1/1/2	1/1/2
1	4/5/6	8/7/8	16/9/10	32/11/12	512/19/20
2	9/21/12	27/37/20	81/57/30	243/81/42	19683/217/110
3	16/21/20	64/37/40	256/57/70	1024/81/112	262144/217/440
4	25/73/30	125/161/70	625/289/140	3125/471/252	1953125/1879/1430
5	36/73/42	216/161/112	1296/289/252	7776/471/504	10077696/1879/4004
6	49/73/56	343/161/168	2401/289/420	16807/471/924	40353607/1879/10010
7	64/73/72	512/161/240	4096/289/660	32768/471/1584	134217728/1879/22880
8	81/221/90	729/608/330	6561/1268/990	59049/2341/2574	387420489/13525/48620
9	100/221/110	1000/608/440	10000/1268/1430	100000/2341/4004	100000000/13525/97240
10	121/221/132	1331/608/572	14641/1268/2002	161051/2341/6006	2357947691/13525/184756

affordable for the smallest problems (two random variables or less), but quickly becomes computationally intractable. Point collocation, on the other hand, is more affordable than quadrature for larger problems and higher expansion orders, and is the most affordable overall within a middle ground. Finally, cubature is the most affordable for the largest dimensionalities and expansion orders.

A common occurrence in practice for production engineering uncertainty analysis is the presence of a particular computational budget (e.g., 10, 100, perhaps 1000 simulations) for a UQ problem with a particular dimensionality  $n$ . In these cases, one can be left in the awkward situation of selecting between a TP/SG/PC approach using a lower expansion order than one would like (due to the type of minimum simulation requirements discussed above) or retaining the desired expansion order and resorting to random sampling for the coefficient estimation (since this technique does not enforce any minimum simulation requirements).

The answer to this question of accurate expansion of lower order vs. inaccurate expansion of higher order will be application-dependent in general, as dictated by the truncation of critical terms in the former case. Thus, an important goal in this work is to lower the barriers to the adoption of the techniques with superior convergence behavior such that the occurrences of this dilemma can be minimized.

## G. Elliptic PDE

Consider the model elliptic problem with one spatial dimension,

$$-\frac{\partial}{\partial x} \left( \alpha(x, \xi_0, \dots, \xi_d) \frac{\partial}{\partial x} u(x, \xi_0, \dots, \xi_d) \right) = f, \quad x \in [0, 2\pi] \quad (29)$$

with boundary conditions  $u(0) = u(2\pi) = 0$ . The spatially varying coefficients are given by a function of  $d$  stochastic parameters as

$$\alpha(x, \xi_0, \dots, \xi_d) = 11 + \sum_{i=0}^d \xi_i \cos(\omega_i x),$$

where  $\xi_0, \dots, \xi_d$  are independent and distributed uniformly over the interval  $[-1, 1]$ . The wave numbers are chosen as  $\omega_0 = 1$  and  $\omega_i = i$  for  $i = 1, \dots, d$ .

To verify convergence of the CDF computed with the non-intrusive polynomial chaos method, we manufacture a solution to Eq. 29. We choose

$$\bar{u}(x, \xi_0, \dots, \xi_d) = \left( \sum_{i=0}^d \xi_i^4 \right) \sin(x). \quad (30)$$

We can compute the approximate CDF of  $\bar{u}$  at a particular spatial coordinate  $x^*$  by sampling techniques to get a reference quantity to compare with the results from the non-intrusive polynomial chaos technique. We call the reference quantity the “exact” solution and denote it by  $\text{CDF}_{u(x^*)}$ .

By applying the differential operator of Eq. 29 to  $\bar{u}$ , we generate a “right hand side”  $\bar{f}$  that guarantees that the solution to Eq. 29 is indeed  $\bar{u}$ .

$$\bar{f} \equiv -\frac{\partial}{\partial x} \left( \alpha \frac{\partial}{\partial x} \bar{u} \right) = \left( \sum_{i=0}^d \xi_i^4 \right) \left[ 11 + \cos(x) \left( \sum_{i=0}^d \xi_i \omega_i \sin(\omega_i x) \right) + \sin(x) \left( 1 + \sum_{i=0}^d \xi_i \cos(\omega_i x) \right) \right] \quad (31)$$

We have a short C++ code that implements a Chebyshev spectral method to solve the deterministic analogue of Eq. 29 given  $\xi_0, \dots, \xi_d$ , and  $\bar{f}$ . Using DAKOTA to interface with this code, we employ the non-intrusive polynomial chaos method with the Legendre basis polynomials. We examine two variants of this problem: a three-dimensional variant ( $d = 2$ ) and a ten-dimensional variant ( $d = 9$ ). For the three-dimensional problem, we plot the CDFs computed with both a Gauss quadrature-based tensor grid and a Clenshaw-Curtis-based sparse grid. In the tensor grid case, we approximate the PCE coefficients using quadrature order = 3, 5, and 9 in each coordinate yielding a total of 27, 125, and 729 respective deterministic simulations. In the sparse grid case, we increase the level parameter in the sparse grid algorithm from 2 to 5 when computing the PCE coefficients; the number of deterministic simulations per level is 25, 69, 177, and 441, respectively. These plots are shown in figure 18, where it is evident that the CDF has converged by quadrature order = 5 and cubature level = 4 (at the expense of 125 and 177 evaluations, respectively). For the ten-dimensional problem, the tensor grid method becomes very expensive, so we only compute the CDF for at most a three point rule along each coordinate. The number of deterministic simulations for these computations are 1, 1024, and 59049, respectively. The number of necessary deterministic simulations for the sparse grid computations at levels 1 through 5 are 21, 221, 1581, 8801, and 41265, respectively. These plots are shown in Figure 19, where it is evident that the CDF has not yet converged by quadrature order = 3 (using 59049 evaluations; the required quadrature order = 5 would use 9765625 evaluations), but has converged by cubature level = 4 (using 8801 evaluations).

## V. Conclusions

The coefficients of chaos expansions in non-intrusive polynomial chaos methods can be calculated through Galerkin projection, based on sampling, quadrature, or cubature, or through linear regression analysis.

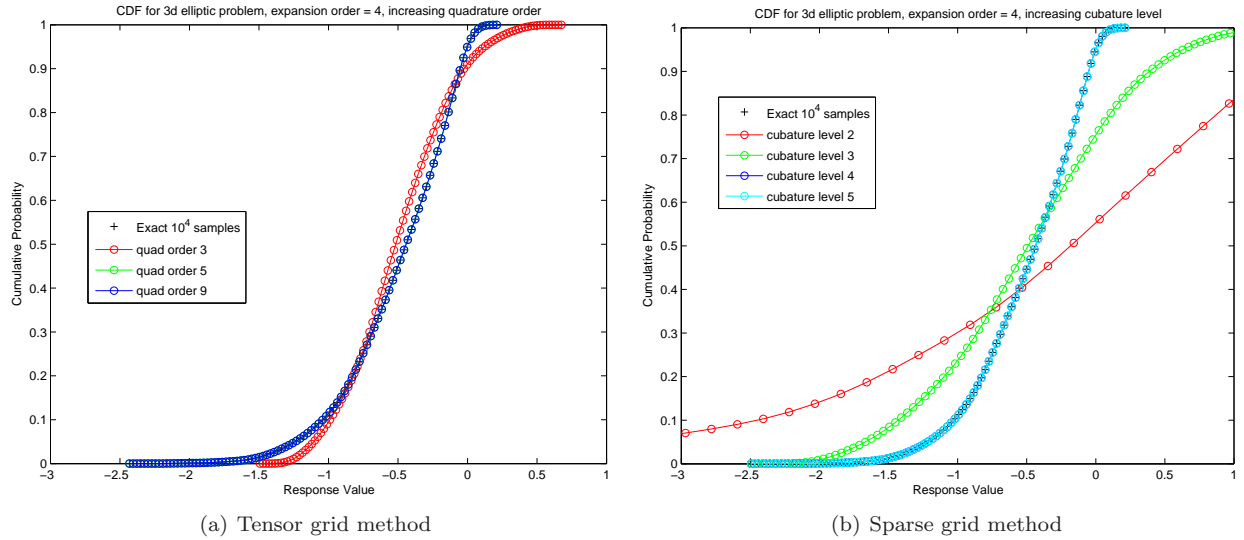


**Figure 18.** CDF of PCE response surface of  $u(x^*)$ , where  $u$  solves the elliptic problem with three random parameters.

This paper has investigated the relative performance of these techniques within Wiener-Askey generalized polynomial chaos approaches applied to algebraic benchmark problems with known solutions and an elliptic PDE problem with a manufactured solution.

UQ results for the first two test problems demonstrated that quadrature, cubature, and regression approaches are to be strongly preferred over sampling, with super-algebraic/exponential convergence rates with respect to simulation evaluation counts for quadrature/cubature/regression, as compared to the well known algebraic rate of  $\frac{1}{2}$  for sampling. The only advantage to the sampling technique is flexibility, in that any number of samples can be selected for coefficient estimation. While the accuracy obtained for a given simulation budget will be much lower for a sampling technique, the simulation requirements imposed by quadrature/cubature/regression may be impractical for the desired expansion order, forcing the undesirable situation of selecting between a quadrature/cubature/regression-based expansion of a lower, affordable order and a sampling-based expansion of the desired order. Thus, lowering the simulation requirements in preferred techniques is clearly desirable so that they are deployable for applications of practical interest.

Within the three higher-performing coefficient estimation approaches, tensor-product quadrature is an excellent technique when analyzing a small number of random variables. Regression, on the other hand, is the most affordable for middle size problems, and sparse grid cubature is preferred for scalability to larger random variable sets. A final important distinction is that quadrature and cubature methods are explicit, whereas point collocation is implicit, requiring a potentially large-scale least squares matrix solution. Numerical ill-conditioning has been observed in some cases involving large sample sets, which appears to be the primary weakness of the regression approach.

Each of the test problems shows excellent accuracy using low-order polynomial chaos expansions, with one exception. When an optimal Askey basis is not available (e.g., for extreme value distributions), distribution transformation techniques used in combination with Askey bases may be insufficient. In particular, the first moment of the expansion for the steel column test problem failed to converge, and the second moment diverged. For these types of problems, additional random discretization (e.g., Refs. 32–34), either to resolve discontinuities or more accurately represent arbitrary input PDFs, may be required.

The current direction of this work is focused on the development of adaptive Wiener-Askey schemes that can tailor the basis, the expansion order, and the numerical integration order to the problem at hand. In addition, stochastic collocation methods are of interest, with the primary distinction of replacing the Askey orthogonal polynomials used in generalized PCE with Lagrange interpolating polynomials. Relative to PCE, these methods hold the advantage of reducing the complexity of the algorithm controls, as expansion order is dictated directly by the integration points and no longer needs to be specified independently.

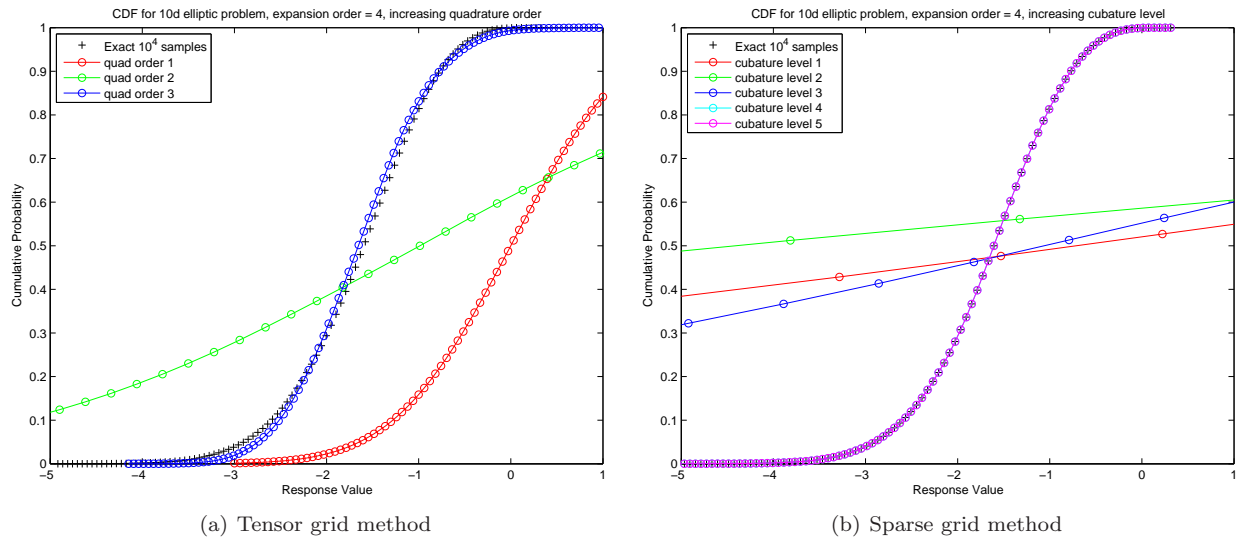


Figure 19. CDF of PCE response surface of  $u(x^*)$ , where  $u$  solves the elliptic problem with ten random parameters.

## Acknowledgments

The authors thank Roger Ghanem, Jianxu Shi, and John Red-Horse for developing the initial Hermite polynomial chaos software in DAKOTA that provided a basis for the Wiener-Askey scheme explored in this work. The authors also thank Rich Field for contribution of the analytic solution for the lognormal ratio test problem, John Burkardt for development of Gauss point/weight and sparse grid software, Rich Field and Habib Najm for helpful comments during the preparation of this manuscript, and the Sandia Computer Science Research Institute (CSRI) for support of this collaborative work between Sandia National Laboratories and Stanford University.

## References

- <sup>1</sup>Xiu, D. and Karniadakis, G. M., "The Wiener-Askey Polynomial Chaos for Stochastic Differential Equations," *SIAM J. Sci. Comput.*, Vol. 24, No. 2, 2002, pp. 619–644.
- <sup>2</sup>Askey, R. and Wilson, J., "Some Basic Hypergeometric Polynomials that Generalize Jacobi Polynomials," *Mem. Amer. Math. Soc.* 319, AMS, Providence, RI, 1985.
- <sup>3</sup>Wiener, N., "The Homogeneous Chaos," *Amer. J. Math.*, Vol. 60, 1938, pp. 897–936.
- <sup>4</sup>Abramowitz, M. and Stegun, I. A., *Handbook of Mathematical Functions with Formulas, Graphs, and Mathematical Tables*, Dover, New York, 1965.
- <sup>5</sup>Eldred, M. S., Agarwal, H., Perez, V. M., Wojtkiewicz, Jr., S. F., and Renaud, J. E., "Investigation of Reliability Method Formulations in DAKOTA/UQ," *Structure & Infrastructure Engineering: Maintenance, Management, Life-Cycle Design & Performance*, Vol. 3, No. 3, 2007, pp. 199–213.
- <sup>6</sup>Eldred, M. S. and Bichon, B. J., "Second-Order Reliability Formulations in DAKOTA/UQ," *Proceedings of the 47th AIAA/ASME/ASCE/AHS/ASC Structures, Structural Dynamics and Materials Conference*, No. AIAA-2006-1828, Newport, RI, May 1–4 2006.
- <sup>7</sup>Rosenblatt, M., "Remarks on a Multivariate Transformation," *Ann. Math. Stat.*, Vol. 23, No. 3, 1952, pp. 470–472.
- <sup>8</sup>Der Kiureghian, A. and Liu, P. L., "Structural Reliability Under Incomplete Probability Information," *J. Eng. Mech., ASCE*, Vol. 112, No. 1, 1986, pp. 85–104.
- <sup>9</sup>Box, G. E. P. and Cox, D. R., "An Analysis of Transformations," *J. Royal Stat. Soc.*, Vol. 26, 1964, pp. 211–252.
- <sup>10</sup>Rackwitz, R. and Fiessler, B., "Structural Reliability under Combined Random Load Sequences," *Comput. Struct.*, Vol. 9, 1978, pp. 489–494.
- <sup>11</sup>Chen, X. and Lind, N. C., "Fast Probability Integration by Three-Parameter Normal Tail Approximation," *Struct. Saf.*, Vol. 1, 1983, pp. 269–276.
- <sup>12</sup>Wu, Y.-T. and Wirsching, P. H., "A New Algorithm for Structural Reliability Estimation," *J. Eng. Mech., ASCE*, Vol. 113, 1987, pp. 1319–1336.
- <sup>13</sup>Ghanem, R. G., private communication.
- <sup>14</sup>Nobile, F., Tempone, R., and Webster, C. G., "A Sparse Grid Stochastic Collocation Method for Partial Differential Equations with Random Input Data," *SIAM J. on Num. Anal.*, 2008, To appear.

- <sup>15</sup>Nobile, F., Tempone, R., and Webster, C. G., “An Anisotropic Sparse Grid Stochastic Collocation Method for Partial Differential Equations with Random Input Data,” *SIAM J. on Num. Anal.*, 2008, To appear.
- <sup>16</sup>Gerstner, T. and Griebel, M., “Numerical integration using sparse grids,” *Numer. Algorithms*, Vol. 18, No. 3-4, 1998, pp. 209–232.
- <sup>17</sup>Smolyak, S., “Quadrature and interpolation formulas for tensor products of certain classes of functions,” *Dokl. Akad. Nauk SSSR*, Vol. 4, 1963, pp. 240–243.
- <sup>18</sup>Barthelmann, V., Novak, E., and Ritter, K., “High dimensional polynomial interpolation on sparse grids,” *Adv. Comput. Math.*, Vol. 12, No. 4, 2000, pp. 273–288, Multivariate polynomial interpolation.
- <sup>19</sup>Frauenfelder, P., Schwab, C., and Todor, R. A., “Finite elements for elliptic problems with stochastic coefficients,” *Comput. Methods Appl. Mech. Engrg.*, Vol. 194, No. 2-5, 2005, pp. 205–228.
- <sup>20</sup>Xiu, D. and Hesthaven, J., “High-order collocation methods for differential equations with random inputs,” *SIAM J. Sci. Comput.*, Vol. 27, No. 3, 2005, pp. 1118–1139 (electronic).
- <sup>21</sup>Wasilkowski, G. W. and Woźniakowski, H., “Explicit Cost Bounds of Algorithms for Multivariate Tensor Product Problems,” *Journal of Complexity*, Vol. 11, 1995, pp. 1–56.
- <sup>22</sup>Babuška, I. M., Tempone, R., and Zouraris, G. E., “Galerkin finite element approximations of stochastic elliptic partial differential equations,” *SIAM J. Numer. Anal.*, Vol. 42, No. 2, 2004, pp. 800–825.
- <sup>23</sup>Babuška, I., Nobile, F., and Tempone, R., “A stochastic collocation method for elliptic partial differential equations with random input data,” *SIAM J. Numer. Anal.*, Vol. 43, No. 3, 2007, pp. 1005–1034.
- <sup>24</sup>Walters, R. W., “Towards Stochastic Fluid Mechanics via Polynomial Chaos,” *Proceedings of the 41st AIAA Aerospace Sciences Meeting and Exhibit*, No. AIAA-2003-0413, Reno, NV, January 6–9, 2003.
- <sup>25</sup>Hosder, S., Walters, R. W., and Balch, M., “Efficient Sampling for Non-Intrusive Polynomial Chaos Applications with Multiple Uncertain Input Variables,” *Proceedings of the 48th AIAA/ASME/ASCE/AHS/ASC Structures, Structural Dynamics, and Materials Conference*, No. AIAA-2007-1939, Honolulu, HI, April 23–26, 2007.
- <sup>26</sup>Eldred, M. S., Brown, S. L., Adams, B. M., Dunlavy, D. M., Gay, D. M., Swiler, L. P., Giunta, A. A., Hart, W. E., Watson, J.-P., Eddy, J. P., Griffin, J. D., Hough, P. D., Kolda, T. G., Martinez-Canales, M. L., and Williams, P. J., “DAKOTA, A Multilevel Parallel Object-Oriented Framework for Design Optimization, Parameter Estimation, Uncertainty Quantification, and Sensitivity Analysis: Version 4.1 Users Manual,” Tech. Rep. SAND2006-6337, Sandia National Laboratories, Albuquerque, NM, 2007.
- <sup>27</sup>Eldred, M. S., Webster, C. G., and Constantine, P., “Design Under Uncertainty Employing Wiener-Askey Generalized Polynomial Chaos,” to appear in *Proceedings of the 12th AIAA/ISSMO Multidisciplinary Analysis and Optimization Conference*, No. AIAA-2008-6001, Victoria, British Columbia, September 10–12, 2008.
- <sup>28</sup>Schittkowski, K., *More Test Examples for Nonlinear Programming, Lecture Notes in Economics and Mathematical Systems*, Vol. 282, Springer-Verlag, Berlin, 1987.
- <sup>29</sup>Kuschel, N. and Rackwitz, R., “Two Basic Problems in Reliability-Based Structural Optimization,” *Math. Method Oper. Res.*, Vol. 46, 1997, pp. 309–333.
- <sup>30</sup>Sues, R., Aminpour, M., and Shin, Y., “Reliability-Based Multidisciplinary Optimization for Aerospace Systems,” *Proceedings of the 42nd AIAA/ASME/ASCE/AHS/ASC Structures, Structural Dynamics, and Materials Conference*, No. AIAA-2001-1521, Seattle, WA, April 16–19, 2001.
- <sup>31</sup>Wu, Y.-T., Shin, Y., Sues, R., and Cesare, M., “Safety-Factor Based Approach for Probability-Based Design Optimization,” *Proceedings of the 42nd AIAA/ASME/ASCE/AHS/ASC Structures, Structural Dynamics, and Materials Conference*, No. AIAA-2001-1522, Seattle, WA, April 16–19, 2001.
- <sup>32</sup>Wan, X. and Karniadakis, G. M., “Multi-Element Generalized Polynomial Chaos for Arbitrary Probability Measures,” *SIAM J. Sci. Comput.*, Vol. 28, No. 3, 2006, pp. 901–928.
- <sup>33</sup>Wan, X. and Karniadakis, G. M., “Beyond Wiener-Askey Expansions: Handling Arbitrary PDFs,” *Journal of Scientific Computing*, Vol. 27, No. 1, 2006.
- <sup>34</sup>Le Maitre, O. P., Knio, O. M., Najm, H. N., and Ghanem, R. G., “Uncertainty propagation using Wiener-Haar expansions,” *Journal of Computational Physics*, Vol. 197, 2004.